Improved Waveforms for Time-Efficient Radar Range Measurement Disambiguation

Alexander Michael Daniel
Radar Sensing and Exploitation Section
Defence Research and Development Canada
Ottawa, Canada, K1A 0Z4
Alexander.Daniel@drdc-rddc.gc.ca

***Abstract*—Ambiguity in radar measurements is a well-studied problem, but more recent advances in multifunction phased-array radars motivate the development of disambiguation schemes that operate in a minimal amount of time. To that end, a recent work has developed a disambiguation scheme that can be optimized to minimize dwell time, but uses waveforms that may degrade the probability of false alarm and result in the masking of small targets. In this paper, we develop several waveform design methods, along with the corresponding optimization framework, for the purpose of mitigating these issues in the case where target velocity is small or known in advance. We show that while some improvement is possible with no increase in dwell time using interpulse codes, substantial improvement can be had with only a mild increase in dwell time by adding CPI separation or mismatched filters, and a perfect response can be obtained by using codes with perfect periodic autocorrelations, but with a more substantial increase in dwell time.**

***Index Terms*—Radar measurement ambiguity, Dwell time minimization, Interpulse codes, Sidelobe ratios, Optimization**

I. Introduction

Ambiguity in range and Doppler measurements is a fundamental problem for pulse-Doppler radars [1]: the unambiguous range, R_{max}, is proportional to the pulse repetition interval (PRI), while the unambiguous velocity, v_{max} is inversely proportional to the PRI. The literature on schemes that can achieve both a large R_{max} and a large v_{max} has been growing for decades; see [2] for a more in-depth review. One common approach uses multiple carefully-selected PRIs to recover the desired data unambiguously; research in these approaches typically focuses selecting the PRIs so as to optimize some quantity of interest, e.g. radar visibility, as in [3]–[5]. Another common approach exploits diverse waveforms: see e.g. [6]–[9], where unique pulses facilitate signal processing techniques that alleviate range ambiguity. However, little attention has been paid to the time-efficiency of these schemes: a technique providing significant improvement beyond a baseline may nevertheless be impractical if the time required to execute it is prohibitively large. A modern phased-array radar may be tasked with multiple functions (e.g. surveillance, tracking, fire control, etc.) [1], and so it is imperative that each task be executed in minimal time so that all functions have sufficient time to be completed. Moreover, for some functions, overall performance can be contingent on the time each task takes, e.g. in surveillance, where better performance is obtained if the radar can revisit each beam position more frequently.

In recent work [2], we developed a disambiguation method that combines the multiple-PRI and diverse waveform approaches described above, paired with an optimization problem, that seeks to provide unambiguous measurements for specified values of R_{max} and v_{max} in minimal time, for fixed values of the probability of false alarm and probability of detection for a specfied target size (see Section II). Some limitations of the scheme, identified in [2], stem from the use of chaotic phase-coded (CPC) waveforms, which, despite having relatively good auto- and cross-correlations on average, can degrade the probability of false-alarm with large spurious recurrent sidelobes and result in the masking of small targets by the recurrent sidelobes of larger targets in multi-target scenarios. The goal of this paper is to develop waveforms for use in the scheme of [2] that mitigate these issues at the expense of an increase in dwell time. Section II reviews the scheme developed in [2], while Section III discusses the waveform design methods. Section IV then compares the relative performance of the methods, while Section V concludes the paper.

II. Review of [2]

This section summarizes the relevant results from [2]; some details are omitted here for the sake of brevity, but the discussion can be found in full there.

Consider a monostatic radar transmitting N pulses per coherent processing interval (CPI), for M such intervals in a single dwell, with the PRI in the i-th CPI is denoted by t_i. Each pulse is a distinct phase-coded waveform with N_c elements of length τ_c each, for a total pulse duration $N_c\tau_c$, where the phase codes are obtained from a chaotic process (specifically a logistic map with a parameter value of 4, following [10]). In principle, this system can achieve an unambiguous range and velocity of R_{max} and v_{max} in the following way. Each pulse has a matched filter that filters all receiver data from the moment that pulse is transmitted to $2R_{max}/c > t_i$ seconds later, i.e. enough time for a pulse reflecting off a target at a distance of R_{max} to return. In principle, the favourable autocorrelation properties of chaotic phase codes means that

©Her Majesty the Queen in Right of Canada, Department of National Defence, 2019

978-9-0827-9703-9/19/$31.00 ©2019 IEEE

any target will show up in the filtered returns as a thumbtack-like spike, while the near-zero cross correlations of different chaotic phase codes will preclude other pulses from showing up as false targets (see [10] for further discussion). With the range ambigutiy gone, the PRIs can be selected to satisfy $t_i^{-1} = f_i \geq 4v_{max}/\lambda$ for an unambiguous velocity of v_{max} [1].[1]

This approach allows for a combination of positive attributes from both the multiple-PRI and diverse waveform approaches discussed in the previous section. With multiple PRIs, the scheme allows for radar visibilitiy as a design parameter, while in typical diverse waveform approaches, visibility is fixed automatically by the pulse length and PRI. On the other hand, the use of diverse waves decouples the range and velocity disambiguation procedures, allowing for greater flexibility in parameter selection. Crucially, this scheme functions for a large set of parameter values (i.e. M, N, N_c, τ_c and the t_i), and so allows for the total dwell time of the scheme to be optimized in terms of those parameters, as in (1a)-(1i).[2]

Equation (1a) gives the dwell time: N pulses separated by the PRI t_i for each CPI, with the final CPI required to wait for the final pulse to return to complete the dwell. Next, (1b) bounds τ_c below with the bandwidth B and the a constant δ representing the clock speed of the computer (following [3]–[5]), while (1c) enforces a maximum duty cycle $\tau_{d,max}$; the meaning of (1d) has been given previously. The function V_κ computes the radar visibility in terms of eclipsing: if a radar is transmitting, it cannot receive data, and so (1e) ensures that a fraction $\zeta \in (0, 1)$ of the desired range is not eclipsed.[3] Using a Neyman-Pearson detector, (1f) fixes a minimum probability of detection P_D for a specified probability of false alarm P_{FA} within a CPI, which are related to "overall" probabilities P_{D_O} and P_{FA_O} by the 2-of-M binary integration rule (for M $\geq$ 3) and a 1-of-M rule if $M \leq 2$; see Table I for parameter definitions. Finally, (1g) mitigates range migration by ensuring the range resolution is larger enough to accomodate a target traveling at v_{max} within one CPI, while (1h)-(1i) model discrete times representable in a computer.

This optimization problem can be solved effectively with a branch and bound method: a analytically-solvable convex subproblem provides the lower bound, while the algorithm branches over N and N_c. For a given N and N_c a simple search procedure is used to find good t_i and τ_c values.

Simulations were run to determine the efficacy of this disambiguation scheme. While most simulations worked as desired, two salient limitations were identified: the recurrent sidelobes of the CPC waves are prone to spurious spikes that can trigger false alarms and have a "volume" that increase the chances of masking smaller targets. In the next section, we will develop methods that, at the expense of increased dwell time, mitigate these issues substantially.

$$\min_{\{a_i\},b,N,N_c} \quad t_D = \sum_{i=1}^{M} N t_i - t_M + N_c\tau_c + 2R_{max}/c \tag{1a}$$

$$\text{s.t.} \quad \tau_c \geq \max\{1/B, \delta\}, \tag{1b}$$

$$N_c\tau_c \leq \tau_{d,max} \min_i\{t_i\}, \tag{1c}$$

$$\max\{t_i\} \leq \frac{\lambda}{4v_{max}}, \tag{1d}$$

$$V_\kappa(N, N_c, \{t_i\}_{i=1}^M) \geq \zeta, \tag{1e}$$

$$Q\left(Q^{-1}\left(P_{FA}\right) - \sqrt{\frac{2P_t G^2\lambda^2\sigma_0\kappa N N_c\tau_c}{(4\pi)^3 R_{max}^4 k T_0 F L_s}}\right) \geq P_D, \tag{1f}$$

$$v_{max} \max_i\{t_i\}N \leq \frac{c\tau_c}{2}, \tag{1g}$$

$$\tau_c = b\delta,\ t_i = a_i\tau_c,\ \forall i \in \{1, \ldots, M\}, \tag{1h}$$

$$a_i,\ b,\ N,\ N_c \in \mathbb{Z}^+ \tag{1i}$$

III. Waveform Design Methods

The main method of developing improved waveforms here will be through the use of interpulse codes (see e.g. [9] and Section 9.1 of [11]). Simple arguments (omitted for brevity) show that if identical pulses are used in the scheme outlined above, with each successive pulse multiplied by the next (complex, unit magnitude) term in a given phase code, then after matched-filtering, the n-th recurrent sidelobe is multiplied by the n-th tap of the autocorrelation of that code. Thus, by choosing an interpulse code with very low autocorrelation sidelobes, the recurrent lobes of the original waveform will be substantially reduced. Note that, as in [9] and [12], the use of phase codes limits the focus here to range disambiguation in cases where target velocity is close to zero or known *a priori*; while this condition is limiting in practice, discussion on more general extensions is given in Section IV.

A. Method 1: Basic Interpulse Codes

The most basic approach is to simply use the system described in the previous section as-is, with an interpulse code overlaid on the pulses. The advantage of this kind of approach is that it does not require any additional dwell time to function. The baseline, which we denote *Method 0*, is the use of CPC pulses as described above, without any interpulse code. This will be compared to *Method 1.1*, CPC pulses overlaid with a P4 interpulse code [11], *Method 1.2*, identical P4-coded pulses with a P4 interpulse code, and *Method 1.3*, P4-coded pulses with a near-optimal biphase interpulse code obtained from the following optimization problem using a simple algorithm which takes the best among a large number of randomly-selected, greedily-improved codes:

$$\min_{\mathbf{y}} \sum_{i=1}^{N_r}\left(\sum_{j=1}^{N-i} y(j)y(j+i)\right)^2, \text{ s.t. } \mathbf{y} \in \{-1, +1\}^N \tag{2}$$

[1]Strictly speaking, since the data is being sampled with a period of τ_c (to facilitate the phase codes), the condition is $\tau_c^{-1} \geq 4v_{max}/\lambda$, but it is discussed in [2] that non-negligible recurrent lobes can still appear in the ambiguity function at multiples of t_i^{-1}, so we impose the condition using t_i^{-1} instead of τ_c^{-1}.

[2]Note that (1a)-(1i) assumes a fixed value of M. This optimization problem is run for each candidate value of M to determine the best possible M.

[3]This is in constrast to [3]–[5], which incorporates both eclipsing and clutter into the visibility metric; we consider a noise-only case here.

This problem minimizes magnitude of the autocorrelation of the interpulse code, $\mathbf{y}$, in the taps affecting recurrent lobes in the unambiguous range. The number $N_r = \lceil 2R_{max}/(c\min\{t_i\})\rceil$ gives the maximum number of recurrent lobes in the unambiguous range, and so problem (1a)-(1i) must be solved before (2).

B. Method 2: Interpulse Codes with CPI Separation

As described by (1a), the scheme in [2] does not wait for the pulses of one CPI to return before starting the next, i.e. the first pulse of CPI i is transmitted only t_{i-1} seconds after the beginning of the last pulse of CPI $i-1$. This can cause some degradation of the interpulse code effect: the first few pulses from the next CPI (and the last few pulses of the previous CPI) are integrated with the returns of the current CPI, but don't necessarily line up with the current CPI pulses because each CPI has a different PRI. If, however, $2R_{max}/c$ seconds are allowed to pass between CPI, all pulses from targets up to a range R_{max} away will be returned, and not interfere with the returns of adjacent CPI. The integrated data will have improved recurrent sidelobes at the expense of the added time due to the wait between CPI. This requires a slightly modified optimization problem: (1a)-(1i) are still the constraints, but

$$t_D = \sum_{i=1}^{M} ((N-1)t_i + N_c\tau_c + 2R_{max}/c) \tag{3}$$

is the objective function.[4] This problem can then be solved similarly to (1a)-(1i). *Method 2.1* involves a P4 interpulse code on P4-coded pulses, while *Method 2.2* uses a code obtained from (2) on P4-coded pulses.

C. Method 3: Mismatched Codes

In Method 1, the interpulse code uses a matched filter, but further recurrent sidelobe reduction can be obtained if a mismatched filter (MMF) is used (see Ch. 6, [11]). The mismatched filter results in an signal-to-noise-ratio (SNR) loss (which can be modelled in (1a)-(1i) by increasing the value of the loss term L_s in (1f)), which in turn causes an increase in dwell time to maintain a fixed P_D and P_{FA}. The following convex optimization problem allows for the design of a mismatched filter, $\mathbf{q}$, for a code $\mathbf{s}$ that minimizes the height of specified sidelobes in their cross-correlation [12], [13]:

$$\min_{\mathbf{q}} \quad \mathbf{q}^H A^H \Lambda A \mathbf{q} \tag{4a}$$

$$\text{s.t.} \quad \mathbf{s}^H\mathbf{q} = \mathbf{s}^H\mathbf{s} \tag{4b}$$

$$\mathbf{q}^H\mathbf{q} \le \alpha \mathbf{s}^H\mathbf{s} \tag{4c}$$

Here, A is a matrix containing shifted versions of $\mathbf{s}$ such that $A\mathbf{q}$ computes the cross-correlation of $\mathbf{q}$ and $\mathbf{s}$. Then, Λ is a diagonal matrix of weights allowing the user to specify which taps of the cross-correlation should be minimized; by choosing $\Lambda_{i,i} = 1$ for $i = -N_r, \ldots, -1, 1, \ldots, N_r$ and 0 otherwise, the optimal code for minimizing the N_r recurrent lobes is obtained. Equation (4b) prevents the trivial $\mathbf{q} = \mathbf{0}$ solution, while (4c) forces a maximum SNR drop of $10\log_{10}\alpha$ dB; see [12] and [13] for further details. *Methods 3.1, 3.2,* and *3.3* will involve the use of P4-coded pulses with a P4 interpulse code and a mismatched filter with SNR losses of 0.125, 0.25, and 0.5 dB respectively. The optimization problem is solved using the convex optimization problem solver CVX [14], [15].

D. Method 4: Perfect Periodic Autocorrelation Codes

The final method is an adaptation of the scheme in [9]. By using codes that have a perfect *periodic* autocorrelation (i.e. zero everywhere except at the mainlobe and its periodic duplicates) as the interpulse code, the recurrent lobes can be entirely eliminated [9]. This technique has two sources of added dwell time. First, to avoid boundary effects ruining the perfect period autocorrelation, two additional sequences of the code must be sent [9]. Second, the CPI must be separated as in Method 2. To reflect these changes, some modifications to the optimization problem used for Method 2 must be made. First, replace every instance of N in the problem with $(b_2+2)N_1$ (with $b_2, N_1 \in \mathbb{Z}^+$), except in (1f), where N is replaced with $N_2 \in \mathbb{Z}^+$. Here, N_2 is used to guarantee enough energy is put on target by adding a constraint $b_2N_1 \ge N_2$, while b_2N_1 is the total number of pulses integrated after processing, and $(b_2+2)N_1$ is the total number of pulses transmitted per CPI, reflecting the addition of two additional sequences. Finally, the constraint $N_1 \ge 2R_{max}/(c\min\{t_i\})$ is added to ensure that the interpulse code can eliminate all recurrent lobes. These changes do not have a drastic effect on the solution algorithm: branching (for the branch-and-bound portion) now occurs over N_1, N_2 and N_c, with the first new constraint simply restricting the set of choices for N_1 and N_2, while the second new constraint adds a constant lower bound to $\min\{t_i\}$, which is already bounded below by $N_c\tau_c/\tau_{d,max}$. *Method 4* uses a P4 code as the perfect interpulse code[5] with P4-coded pulses.

IV. Performance Comparison

This section examines how the different waveform design methods improve two different metrics. Let $x(i), i = 1, \ldots, \lceil 2R_{max}/(c\tau_c)\rceil$ be the set of (noiseless) filtered and integrated range samples, and let a target be located in cell j. The first metric, the *peak recurrent sidelobe level* (PRSL),

$$\text{PRSL} = \max_{\forall i \ne j-N_c+1,\ldots,j+N_c-1} \left\{ \left| \frac{x(i)}{x(j)} \right| \right\}$$

is a proxy of how likely recurrent lobes are likely to trigger a false alarm, while the second metric, the *normalized integrated recurrent sidelobe level* (NIRSL),

$$\text{NIRSL} = \frac{1}{N_r}\left(\sum_{i=1}^{j-N_c} \left(\frac{x(i)}{x(j)}\right)^2 + \sum_{i=j+N_c}^{\lceil 2R_{max}/(c\tau_c)\rceil} \left(\frac{x(i)}{x(j)}\right)^2 \right)^{\frac{1}{2}},$$

provides a measure of the degree to which a waveform could mask other targets with its recurrent lobes. The normalization

[4] Note that when $M = 1$, the two optimization problems are equivalent.

[5] Note that, up until now, the P4 code has been used for its *aperiodic* autocorrelation, and is now being used for its perfect periodic autocorrelation [11].

TABLE I
SYSTEM PARAMETERS FOR SIMULATION

Parameter	Symbol	Value
Unamb. Range	R_{max}	23 km
Unamb. Velocity	v_{max}	700 m/s
Overall Prob. of Det.	P_{D_O}	0.9
Overall Prob. of False Alarm	P_{FA_O}	10^{-5}
Center Frequency	f_c	3 GHz
Bandwidth	B	20 MHz
Computer Clock Time	δ	10 ns
Min. Target RCS	σ_0	0.01 m^2
Transmission Power	P_t	5 kW
Antenna Gain	G	30 dB
System Temperature	T_0	293 K
Noise Figure	F	3 dB
System Losses	L_s	0 dB
Maximum Duty Cycle	$\tau_{d,max}$	0.1
Nominal Visibility	ζ	0.95
Visibility Fraction	κ	0.99
Receiver Velocity Res.	$v_{sep} = \lambda f_{sep}/2$	1 m/s
Target Range	r	3,824 m
Target RCS	σ	0.01 m^2
Target Velocity	v	0 m/s

TABLE II
OPTIMIZATION PROBLEM OUTCOMES

Method	t_D (ms)	M	N	N_c	τ_c (ns)	$\{a_i\}$
0, 1	4.643	3	111	10	130	$100, 104, 108$
2	4.805	3	222	13	50	$130, 131, 132$
3.1	4.773	3	110	15	90	$150, 156, 162$
3.2	4.876	3	306	10	50	$100, 103, 106$
3.3	5.154	3	324	10	50	$100, 103, 106$
4	5.859	3	(7, 63)	46	50	$460, 473, 486$

by N_r prevents waveforms from being penalized for having more recurrent lobes in the unambiguous range, which is due more to the dwell time optimization problem than the waveform design method. Note that further consideration of peak and integrated sidelobe levels for the waveform autocorrelation itself are beyond the scope of this paper.

Table I shows the system parameter values, while Table II gives the results from the optimization problem for each method.[6] Figures 1 and 2 show the PRSL and NIRSL (respectively) against dwell time for the first three methods; Method 4 achieves perfect PRSL and NIRSL scores of 0 (i.e. $-\infty$ dB) and so is omitted. Since the CPC pulses are generated by random seeds, the results for Methods 0 and 1.1 are taken as the average over 100 Monte Carlo trials, with the minimum and maximum results indicated by the error bars, while all other design methods are deterministic.

Comparing Method 0 to Method 1.3, roughly 10 dB in PRSL and 13 dB in NIRSL of improvement is obtained "for free" by using a good interpulse code. Method 2 can give up to roughly 15 dB and 23 dB improvement in PRSL and NIRSL respectively with only a 3.5% increase in dwell time, while for a slightly larger increase in dwell time (5%), the

[6]For Method 4, the fourth column shows (N_1, N_2). Note that in practice, a constraint $N_c \geq N_{c,min} = 10$ is added to ensure that the autocorrelation has sufficiently good sidelobes.

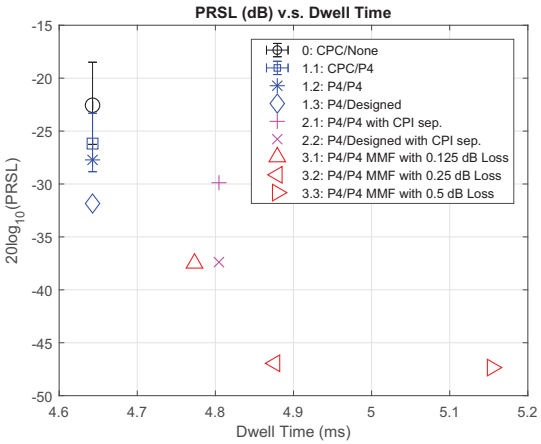

Fig. 1. The tradeoff between PRSL and dwell time.

0.25 dB MMF provides roughly an additional 25 dB PRSL and 25 dB NIRSL. The impact of CPI separation can be seen by comparing Methods 1.2 to 2.1, and 1.3 to 2.2. A few dB are gained in PRSL, but nearly 10 dB in NISRL (for the latter pair) are obtained (see discussion below). The 0.5 dB MMF barely improves upon the 0.25 dB MMF in both PRSL and IRSL, so with an 11% increase in dwell time over the baseline, is not likely to be practical. For further gains (without hitting the 5.859 ms limit of Method 4), one could combine the MMF approach with CPI separation, although this is beyond our scope. If perfect returns are desired, then Method 4 can be used, but at a cost of a 26% increase in dwell time.

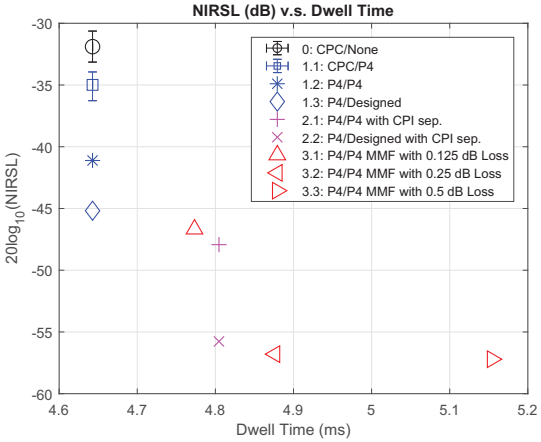

Fig. 2. The tradeoff between NIRSL and dwell time.

Figure 3 provides an illustration of the impact of PRSL and NIRSL improvement by superimposing the normalized range data of three recurrent lobes (from CPI 1) of Method 1.3 on top of that of an instantiation of Method 0. Note how the peaks are drastically reduced (captured by the PRSL metric), making a false alarm less likely, as is the volume occupied by recurrent lobes (captured by the NIRSL metric), which reduces masking. Also note how the height and breadth of the recurrent sidelobes

increase as they get further from the target (not shown, but located at range cell 198). This is due to the fact that the first few pulses of the next CPI are misaligned with pulses from the current CPI becuase of the difference in PRI, and explains why Method 2 achieves such a low NIRSL: it does not have pulses from adjacent CPI interfering. This should also indicate that the results in Figures 1-2 are illustrative rather than definitive: for different system parameters, the dwell time optimization problem outcome (and therefore N_r) might be different, and therefore yield slightly better or worse PRSL and NIRSL values. Nevertheless, the simulation results combined with *a priori* reasoning provide confidence that these results are representative.

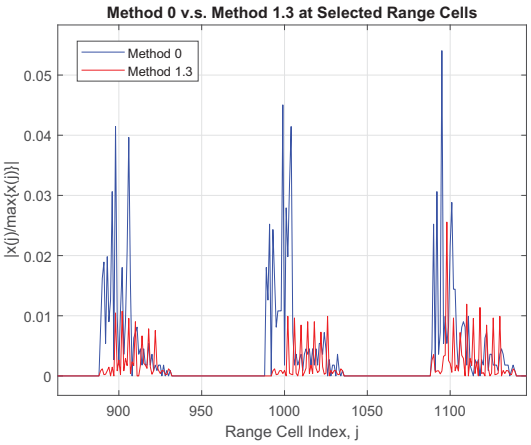

Fig. 3. Comparing the recurrent sidelobes of Method 0 and Method 1.3. The data is normalized so that the autocorrelation mainlobe has a height of 1.

Finally, we note that the Doppler sensitivity of phase codes in Methods 1.3, 2, and 3, render them impractical for cases where the Doppler shift of the target is significant.[7] For Method 0 and 1.1, the CPC pulses have sidelobe behaviour that is (qualitatively) fairly stable across Doppler shifts, which is the property that allowed Method 0 to be used in [2]; limitations of space prevent the full ambiguity functions from being shown here, however. Moreover, Methods 1.2 and 4 use identical pulses with a P4 interpulse code, which is more robust to Doppler shifts [1], resulting in an otherwise-flat ambiguity function with replications of the mainlobe at locations determined by the interpulse code ambiguity function. In principle, this could form the basis of a velocity-disambiguation algorithm similar to standard "coincidence" algorithms [1], although with the modification that the mainlobe replicas in Doppler are not in the same range bin as the target. The development of such a scheme, however, is left to future work.

V. Conclusion

Recent work on time-efficient radar measurement disambiguation [2] employed waveforms that had the potential to degrade the desired probability of false alarm and mask the returns of smaller targets. This work introduced a number of techniques for mitigating these issues in the case where target velocities are small or known in advance, and showed how to modify the optimization framework of [2] to minimize the dwell time for each technique. It was shown that notable improvement could be obtained (without increasing dwell time) by using an appropriate interpulse phase code. Further, using CPI separation and mismatched filters for the interpulse codes yielded additional gains, at the expense of a small increase in dwell time (approximately 3.5% and 5% respectively). While a perfect response could be obtained exploiting phase codes with a perfect periodic autocorrelation, the cost of this was a 26% increase in dwell time. Nevertheless, such an approach may be necessary to develop a scheme capable of accomodating large target velocities, which is the aim of future research.

[7]The value of v_{max} in Table I is the value used in the various optimization problems, but is not the value up to which these methods are valid.

References

[1] M. A. Richards, J. A. Scheer, and W. A. Holm, Eds., *Principles of Modern Radar: Basic Principles*. SciTech Publishin, 2010.

[2] A. M. Daniel, "Dwell time minimization for unambiguous radar range and doppler measurements," Ottawa Research Center, Defence Research and Development Canada, Tech. Rep. DRDC-RDDC-2019-R006, 2019, In Press. [Online]. Available: http://pubs.drdc-rddc.gc.ca/

[3] P. G. Davies and E. J. Hughes, "Medium PRF set selection using evolutionary algorithms," *IEEE Transactions on Aerospace and Electronic Systems*, vol. 38, no. 3, pp. 933–939, Jul 2002.

[4] C. M. Alabaster, E. J. Hughes, and J. H. Matthew, "Medium PRF radar PRF selection using evolutionary algorithms," *IEEE Transactions on Aerospace and Electronic Systems*, vol. 39, no. 3, pp. 990–1001, July 2003.

[5] D. Wiley, S. Parry, C. Alabaster, and E. Hughes, "Performance comparison of PRF schedules for medium PRF radar," *IEEE Transactions on Aerospace and Electronic Systems*, vol. 42, no. 2, pp. 601–611, April 2006.

[6] J. M. Anderson, M. A. Temple, W. M. Brown, and B. L. Crossley, "A nonlinear suppression technique for range ambiguity resolution in pulse doppler radars," in *Proceedings of the 2001 IEEE Radar Conference (Cat. No.01CH37200)*, 2001, pp. 141–146.

[7] J. Kurian, M. A. Temple, M. J. Papaphotis, and W. M. Brown, "Mutually dispersive pulse coding to enhance non-linear ambiguity suppression," in *2003 Proceedings of the International Conference on Radar (IEEE Cat. No.03EX695)*, Sept 2003, pp. 694–699.

[8] J. D. Jenshak and J. M. Stiles, "Transmit coding with a range ambiguity," in *2009 International Waveform Diversity and Design Conference*, Feb 2009, pp. 98–102.

[9] N. Levanon, "Mitigating range ambiguity in high PRF radar using interpulse binary coding," *IEEE Transactions on Aerospace and Electronic Systems*, vol. 45, no. 2, pp. 687–697, April 2009.

[10] X. Wu, W. Liu, L. Zhao, and J. S. Fu, "Chaotic phase code for radar pulse compression," in *Proceedings of the 2001 IEEE Radar Conference (Cat. No.01CH37200)*, May 2001, pp. 279–283.

[11] N. Levanon and E. Mozeson, *Radar Signals*. Hoboken, NJ, USA: Wiley, 2004.

[12] O. Rabaste and L. Savy, "Mismatched filter optimization for radar applications using quadratically constrained quadratic programs," *IEEE Transactions on Aerospace and Electronic Systems*, vol. 51, no. 4, pp. 3107–3122, Oct 2015.

[13] K. R. Griep, J. A. Ritcey, and J. J. Burlingame, "Poly-phase codes and optimal filters for multiple user ranging," *IEEE Transactions on Aerospace and Electronic Systems*, vol. 31, no. 2, pp. 752–767, April 1995.

[14] M. Grant and S. Boyd, "CVX: Matlab software for disciplined convex programming, version 2.1," http://cvxr.com/cvx, Mar. 2014.

[15] ——, "Graph implementations for nonsmooth convex programs," in *Recent Advances in Learning and Control*, ser. Lecture Notes in Control and Information Sciences, V. Blondel, S. Boyd, and H. Kimura, Eds. Springer-Verlag Limited, 2008, pp. 95–110.